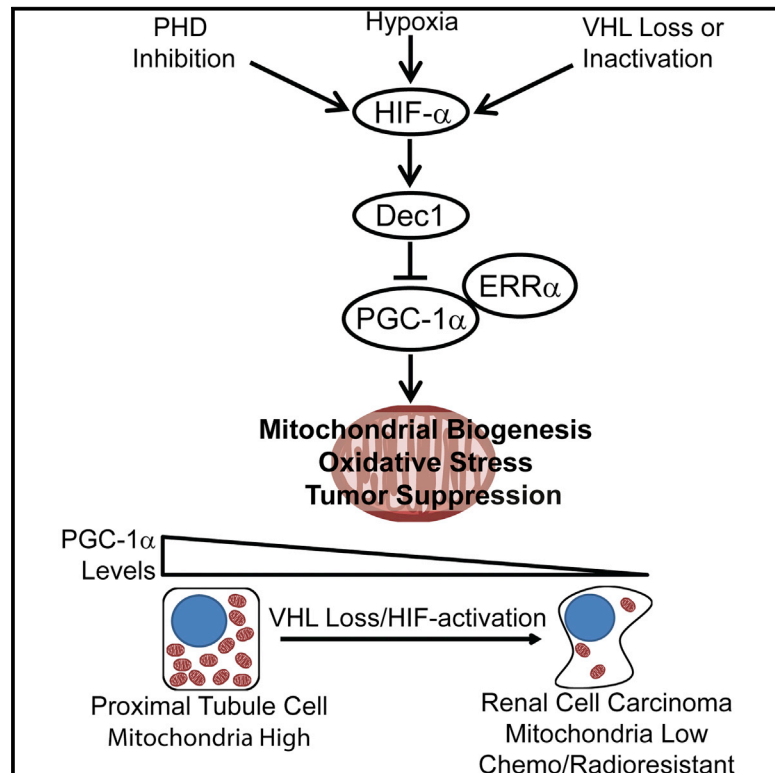**Article**

Suppression of PGC-1α Is Critical for Reprogramming Oxidative Metabolism in Renal Cell Carcinoma

Graphical Abstract

Authors

Edward L. LaGory, Colleen Wu,
Cullen M. Taniguchi, ..., David A. Scott,
Adam D. Richardson, Amato J. Giaccia

Correspondence

giaccia@stanford.edu

In Brief

LaGory et al. show that PGC-1α expression is suppressed in ccRCC in a HIF-α- and Dec1-dependent manner. Rescued expression of PGC-1α restores mitochondrial function, induces oxidative stress, and suppresses tumor growth. In patients, low expression of PGC-1α is associated with poor overall survival and advanced-stage metastatic disease.

Highlights

- PGC-1α suppression reprograms mitochondrial metabolism in ccRCC

- PGC-1α repression is HIF dependent and requires induction of the HIF target gene Dec1

- PGC-1α expression induces oxidative stress and suppresses ccRCC tumor growth

- Low PGC-1α expression is a marker of poor prognosis in ccRCC

CellPress

Suppression of PGC-1α Is Critical for Reprogramming Oxidative Metabolism in Renal Cell Carcinoma

Edward L. LaGory,[1] Colleen Wu,[1] Cullen M. Taniguchi,[1,4] Chien-Kuang Cornelia Ding,[2] Jen-Tsan Chi,[2] Rie von Eyben,[1] David A. Scott,[3] Adam D. Richardson,[3] and Amato J. Giaccia[1,*]

[1]Division of Radiation and Cancer Biology, Department of Radiation Oncology, Stanford University, Stanford, CA 94305, USA
[2]Duke Center for Genomic and Computational Biology, Department of Molecular Genetics and Microbiology, Duke University Medical Center, Durham, NC 27708, USA
[3]NCI-Designated Cancer Center, Sanford Burnham Medical Research Institute, La Jolla, CA 92037, USA
[4]Present address: University of Texas MD Anderson Cancer Center, 1515 Holcombe Boulevard, Houston, TX 77030-4000, USA
*Correspondence: giaccia@stanford.edu
http://dx.doi.org/10.1016/j.celrep.2015.06.006

SUMMARY

Long believed to be a byproduct of malignant transformation, reprogramming of cellular metabolism is now recognized as a driving force in tumorigenesis. In clear cell renal cell carcinoma (ccRCC), frequent activation of HIF signaling induces a metabolic switch that promotes tumorigenesis. Here, we demonstrate that PGC-1α, a central regulator of energy metabolism, is suppressed in VHL-deficient ccRCC by a HIF/Dec1-dependent mechanism. In VHL wild-type cells, PGC-1α suppression leads to decreased expression of the mitochondrial transcription factor Tfam and impaired mitochondrial respiration. Conversely, PGC-1α expression in VHL-deficient cells restores mitochondrial function and induces oxidative stress. ccRCC cells expressing PGC-1α exhibit impaired tumor growth and enhanced sensitivity to cytotoxic therapies. In patients, low levels of PGC-1α expression are associated with poor outcome. These studies demonstrate that suppression of PGC-1α recapitulates key metabolic phenotypes of ccRCC and highlight the potential of targeting PGC-1α expression as a therapeutic modality for the treatment of ccRCC.

INTRODUCTION

First observed by Otto Warburg in the early 20th century, metabolic reprogramming is now accepted as an emerging hallmark of cancer (Hanahan and Weinberg, 2011). Constitutive activation of hypoxia inducible factor (HIF) signaling and accumulation of cytosolic lipid droplets indicate profound changes in cellular metabolism take place during clear cell renal cell carcinoma (ccRCC) tumorigenesis. Indeed, the signaling networks that regulate metabolic behavior are frequently altered in ccRCC, leading to the description of this tumor type as a "metabolic disease" (Linehan et al., 2010). Despite the seemingly important role

of altered metabolism in ccRCC tumorigenesis, the molecular mechanisms underlying these metabolic shifts are incompletely understood. Clinically, ccRCC is refractory to conventional cytotoxic agents, with therapeutic approaches instead favoring surgery and targeted therapies such as tyrosine kinase inhibitors, mTOR inhibitors, and immunotherapy (Rini et al., 2009). Importantly, the mechanism of resistance to chemo/radiotherapy is poorly understood, and whether altered metabolism influences therapeutic response remains unknown.

Deletions and mutations to the tumor suppressor gene Von Hippel-Lindau (Vhl) are the most frequent genetic alterations in ccRCC (Cancer Genome Atlas Research Network, 2013; Gnarra et al., 1994). The Vhl gene encodes an E3 ubiquitin ligase that is essential for oxygen-dependent regulation of HIF-α transcription factors (Kondo et al., 2002; Maxwell et al., 1999). In normal oxygen conditions, HIF-1α and HIF-2α subunits are hydroxylated on key proline residues by oxygen-dependent prolyl hydroxylases (PHDs), bound by VHL, and rapidly degraded by the proteasome (Ivan et al., 2001; Jaakkola et al., 2001). In hypoxia, prolyl hydroxylation is inhibited, resulting in HIF-α stabilization and dimerization with aryl hydrocarbon receptor nuclear transactivator (ARNT) (Wang et al., 1995). Consequently, VHL loss of function results in constitutive activation of HIF-α, which promotes tumorigenesis through transcriptional activation of genes involved in angiogenesis, invasion, metastasis, and metabolism (Gordan and Simon, 2007).

Constitutive activation of HIF transcription factors is thought to be a primary driving force of metabolic reprogramming in ccRCC. HIF transcription factors activate a gene expression program that upregulates glycolytic flux while simultaneously inhibiting mitochondrial activity (Fukuda et al., 2007; Papandreou et al., 2006). The ability of HIF to negatively regulate mitochondrial activity fits with the evolutionary need for coupling oxygen consumption in the mitochondria to nutrient and oxygen availability. In ccRCC, mitochondrial content is inversely correlated with tumor grade, indicating that suppression of mitochondrial activity may play an important role in ccRCC progression (Simonnet et al., 2002). Importantly, the mechanism underlying suppression of mitochondrial content in ccRCC, and the consequences thereof, remain incompletely understood.

The PPARγ coactivators (PGC) are a family of transcriptional coactivators that are regulated by a wide range of environmental stimuli to coordinate mitochondrial biogenesis and metabolic flux (Puigserver et al., 1998). While the PGC coactivators (consisting of PGC-1α, PGC-1β, and PRC) exhibit some degree of redundancy, PGC-1α-knockout mice exhibit multi-tissue defects in mitochondrial metabolism indicating unique functions for PGC-1α that cannot be compensated for by the other family members (Leone et al., 2005; Lin et al., 2004). Although a growing body of evidence points toward an important role for PGC-1α in cancer, an important dichotomy exists, with reports of pro and anti-tumorigenic effects of PGC-1α expression in different cancer types (D'Errico et al., 2011; Haq et al., 2013; LeBleu et al., 2014; Lim et al., 2014; Vazquez et al., 2013; Yan et al., 2014). A better understanding of the role of PGC-1α in different tumor types and at different stages of tumorigenesis will be important in determining whether this pathway will be amenable to therapeutic intervention.

Past studies indicate that dynamic interplay between the HIF transcription factors and c-Myc can regulate expression of PGC-1β and mitochondrial biogenesis (Zhang et al., 2007). Additionally, hypoxia has been linked to the regulation of PGC-1α in adipose tissue, where hypoxia inhibits SIRT2-mediated deacetylation of PGC-1α (Krishnan et al., 2012). Conversely, PGC-1α-induced oxygen consumption and reactive oxygen species (ROS) production have been reported to stabilize and activate HIFs (O'Hagan et al., 2009; Shoag and Arany, 2010). To this point, it has remained unclear whether PGC-1α expression or activity is modulated in ccRCC and, if so, what effect this regulation would have on the metabolic phenotypes and tumorigenic potential of ccRCC.

RESULTS

Suppression of Mitochondrial Biogenesis Transcription Factors in ccRCC

To explore the gene expression changes underlying metabolic alteration in ccRCC, we analyzed previously published microarray datasets from ccRCC cell lines and tumors. Gene set enrichment analysis (GSEA) revealed significant enrichment of hypoxia gene sets and depletion of β-oxidation and tricarboxylic acid (TCA) cycle gene sets in ccRCC compared to the non-malignant kidney (Figures 1A, S1A, and S1B). Furthermore, Database for Annotation, Visualization, and Integrated Discovery (DAVID) analysis revealed suppression of genes involved in mitochondrial function in VHL-deficient ccRCC cells in vitro (Figures 1B and S1C). We hypothesized that these changes in gene expression might result from suppression of the key transcriptional regulators of mitochondrial biogenesis.

Mitochondrial biogenesis is controlled by a network of nuclear transcription factors and coactivators that include the nuclear respiratory factors (NRFs), the estrogen-related receptors (ERRs), and the PGC family of transcriptional coactivators. To determine whether differential expression of these transcriptional regulators could explain the gene expression changes outlined above, we profiled the expression of several genes known to act as regulators of these pathways. To our surprise, PGC-1α, but not PGC-1β, was highly suppressed in ccRCC (Figures 1C, S2A,

and S2B). Additionally, expression of the mitochondrial transcription factor Tfam (a known target of PGC-1α) was decreased in ccRCC, as was ERRα, a transcription factor through which PGC-1α function is transduced (Mootha et al., 2004) (Figure 1C). Consistent with these data, PGC-1α mRNA and protein were suppressed in several VHL-deficient cell lines (Figures 1D–1F and S2C). Given its central role as a regulator of mitochondrial function, we hypothesized that suppression of PGC-1α disrupts mitochondrial content and function in ccRCC.

PGC-1α Is Essential for Mitochondrial Homeostasis in Renal Proximal Tubule Cells

Studies using genetically engineered mouse models indicate that PGC-1α deficiency results in defective mitochondrial metabolism in multiple tissue types (Leone et al., 2005). Similarly, VHL-deficient ccRCC cell lines exhibit HIF-dependent decreases in mitochondrial content and activity (Figures S3A–S3D). We reasoned that the suppression of PGC-1α in VHL-deficient ccRCC could underlie the mitochondrial deficiency characteristic of this cancer type. Consistent with this hypothesis, PGC-1α knockdown in VHL wild-type malignant (TK10) and non-malignant proximal tubule (HK2) cells decreased expression of the essential mitochondrial transcription factor Tfam (Figure 2A). Importantly, PGC-1α suppression also functionally impaired mitochondrial oxygen consumption rates (OCR) in both HK2 and TK10 cells, indicating that endogenous expression of PGC-1α is essential for maintaining basal mitochondrial respiration in these cells (Figures 2B and S3E–S3G). Consistent with impaired mitochondrial function in PGC-1α-deficient cells, gas chromatography-mass spectrometry (GC-MS) analysis revealed significant decreases in TCA cycle metabolite abundance (Figure 2C). These results indicate that PGC-1α expression is essential for mitochondrial function and suggest that suppression of PGC-1α may contribute to the depletion of mitochondrial function observed in ccRCC.

To further explore the role of PGC-1α suppression in ccRCC metabolism, we tested whether restored PGC-1α expression in VHL-deficient cells was sufficient to rescue mitochondrial function (Figure 2D). Consistent with increased mitochondrial content, PGC-1α expression in VHL-deficient RCC4 and 786-O cells increased mtDNA content and CMXRos staining (Figures 2E and S3H). PGC-1α expression also functionally increased mitochondrial respiration in both RCC4 and 786-O cells, an effect that was significantly blunted by withdrawal of exogenous glutamine (Figure 2F). Increased mitochondrial respiration was also partially sensitive to the CPT-1α inhibitor etomoxir, indicating that PGC-1α stimulation of OCR occurred at least in part due to increases in β-oxidation (Figures S3I and S3J). These results provide evidence that restored PGC-1α expression is sufficient to restore mitochondrial content and function in VHL-deficient ccRCC.

PGC-1α function is transduced through interaction with a wide range of nuclear transcription factors, and we next sought to identify the transcription factor(s) acting in concert with PGC-1α to stimulate mitochondrial biogenesis in ccRCC. Using small interfering RNA (siRNA) to transiently suppress expression of several transcription factors known to interact with PGC-1α, we determined that ERRα was required for PGC-1α-induced mitochondrial gene expression in VHL-deficient RCC4 cells
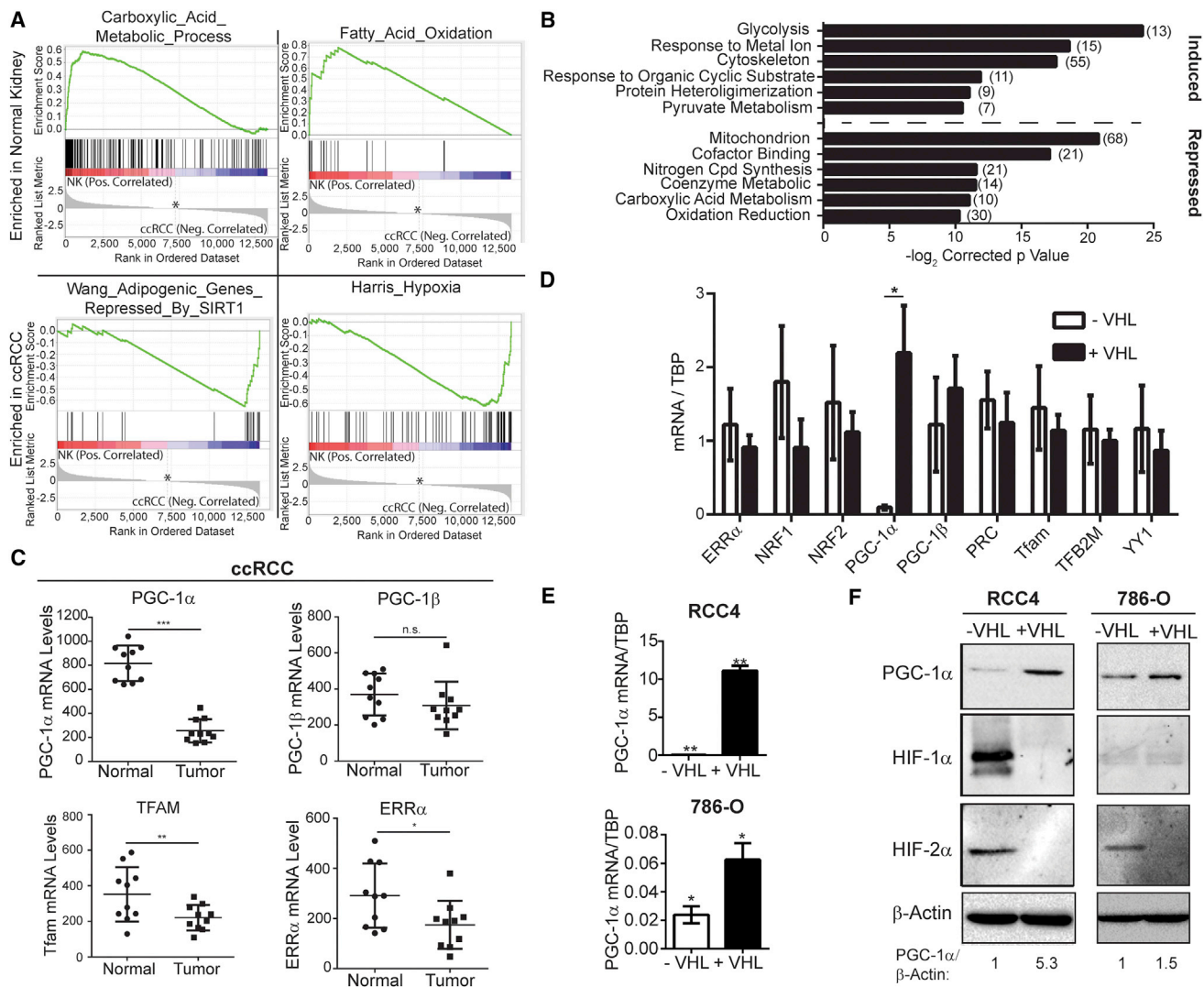
Figure 1. PGC-1α Expression Is Suppressed in VHL-Deficient Clear Cell Renal Cell Carcinoma

(A) GSEA of normal kidney and ccRCC tumors. *Zero cross at 7,239 (GEO:GSE6344).

(B) DAVID analysis of gene expression in RCC4 cells in VHL deficiency or hypoxia. (Array data from Krieg et al., 2010).

(C) mRNA expression levels in normal kidney or ccRCC. Data from GEO:GSE6344. *p < 0.04; **p < 0.03; ***p < 0.0001; n.s., p > 0.05 by Student's two-tailed t test.

(D) mRNA levels in VHL-deficient (−VHL) or wild-type (+VHL) RCC4 cells. *p < 0.0001 by Student's two-tailed t test.

(E) mRNA levels in VHL-deficient (−VHL) or wild-type (+VHL) RCC4 and 786-O cells. *p = 0.01; **p = 0.001 by Student's two-tailed t test.

(F) PGC-1α protein levels in VHL-deficient (−VHL) or wild-type (+VHL) RCC4 and 786-O cells.

All bar graphs are plotted as mean ± SD. See also Figures S1 and S2.

(Figures 2G and S3K). Furthermore, ERRα suppression also abrogated the PGC-1α-increased mitochondrial respiration rate, indicating its essential role as a co-regulator of PGC-1α in regulating mitochondrial function (Figure 2H). These results indicate that ERRα is required for PGC-1α-mediated induction of mitochondrial biogenesis in ccRCC.

PGC-1α Induces Oxidative Stress and Sensitizes ccRCC Cells to Cytotoxic Therapy

ROS are potent byproducts of electron transport chain activity and play a complex role in tumorigenesis. Malignant cells often exhibit elevated steady-state levels of ROS, rendering them

exquisitely sensitive to further increases in ROS production from the mitochondria (Trachootham et al., 2009). We reasoned that the elevated mitochondrial respiratory activity observed upon expression of PGC-1α would likely be accompanied by an increase in ROS production. Furthermore, VHL-deficient ccRCC cell lines exhibit HIF-dependent decreases in both mitochondrial respiration and ROS production, indicating that the two processes are functionally linked (Figures S3C and S4A). In support of this hypothesis, RCC4 and 786-O cells ectopically expressing PGC-1α contained significantly elevated levels of hydroxyl and superoxide radicals as measured by DCF-DA and MitoSOX staining, respectively (Figures 3A, 3B, and S4B). These
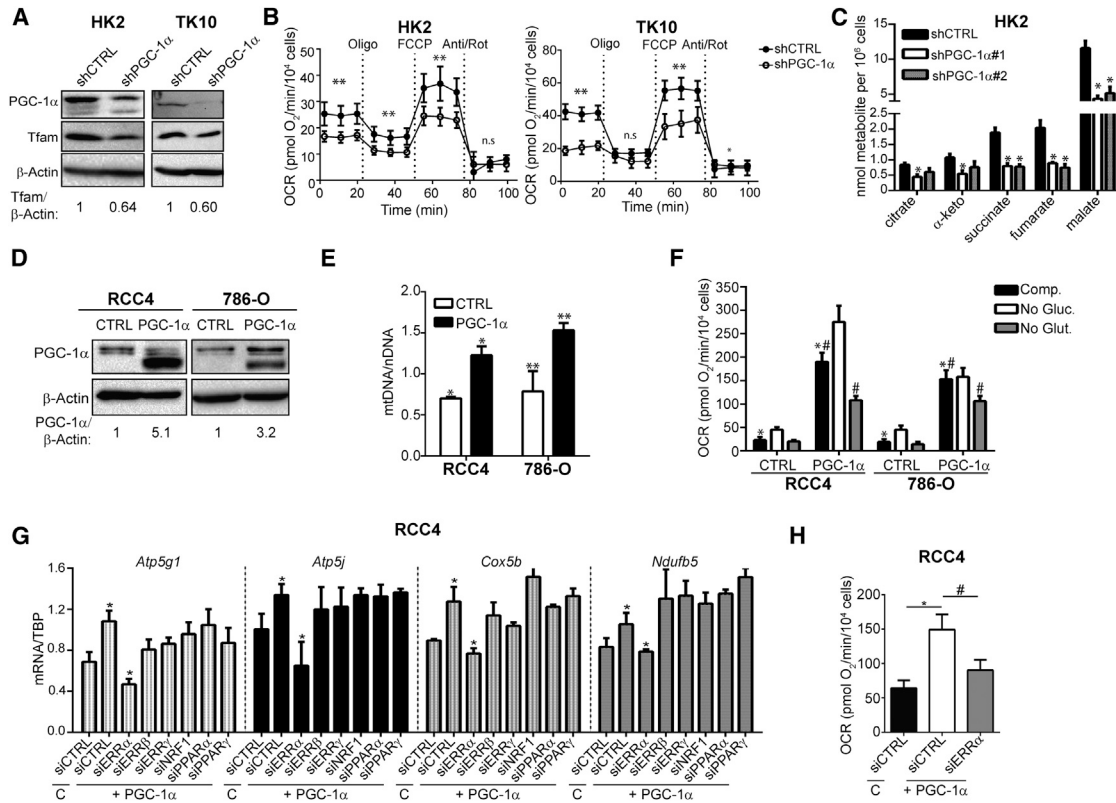
Figure 2. PGC-1α Regulates Mitochondrial Homeostasis and OXPHOS Activity in ccRCC

(A) Western blots of VHL wild-type HK2 and TK10 cells transduced with shCTRL or shPGC-1α.

(B) Oxygen consumption rates (OCRs) in HK2 and TK10 cells transduced with shCTRL or shPGC-1α. Oligomycin (Oligo), FCCP, and antimycin A/rotenone (Anti/Rot) were injected at the indicated time points. Data presented as mean + SEM. Student's two-tailed t test calculated by pooling the three measurements for each condition **$p \leq 0.01$; *$p < 0.05$.

(C) GC-MS quantification of TCA cycle metabolites from shCTRL and shPGC-1α-transduced HK2 cells *$p \leq 0.01$ by Student's two-tailed t test.

(D) Ectopic expression of PGC-1α in VHL-deficient RCC4 and 786-O cells.

(E) mtDNA measurements normalized to nuclear DNA (nDNA) in CTRL or PGC-1α transduced RCC4 and 786-O cells. *$p = 0.01$; **$p < 0.03$ by Student's two-tailed t test.

(F) OCR measurements in CTRL and PGC-1α-transduced RCC4 and 786-O cells cultured with the indicated carbon sources. *,#Two-tailed Student's t test $p < 0.0001$.

(G) qPCR analysis of mitochondrial gene expression in RCC4 cells transduced with control (C) or PGC-1α retrovirus and transfected with the indicated siRNA. *Two-tailed Student's t test $p < 0.05$.

(H) Basal OCR in CTRL and PGC-1α transduced RCC4 cells transfected with the indicated siRNA. *,#Two-tailed Student's t test $p < 0.0001$.

All bar graphs are plotted as mean ± SD unless otherwise noted. See also Figure S3.

results were surprising given the known ability of PGC-1α to coordinate expression of ROS detoxification enzymes with enhanced mitochondrial biogenesis (St-Pierre et al., 2006). Indeed, PGC-1α expression in VHL-deficient cells did increase the expression of several antioxidant genes (Figure 3C). To determine whether the antioxidant response was sufficient to detoxify the observed increases in ROS, we next stained for 8-hydroxyguanosine (8oxoG), an oxidized derivative of guanosine that is commonly used as a biomarker of oxidative stress. Strikingly, both RCC4 and 786-O cells transduced with PGC-1α exhibited significantly elevated levels of 8oxoG compared to control, indicating that PGC-1α expression was sufficient to induce oxidative stress in VHL-deficient ccRCC cells (Figures 3D and S4C). Furthermore, PGC-1α expression increased γH2AX levels in RCC4 cells, indicating the presence of an active

DNA damage response (Figure 3E). These results suggest that PGC-1α-induced mitochondrial activity is tightly associated with oxidative stress in VHL-deficient cells.

ccRCC is resistant to cytotoxic chemotherapy and radio-therapy, and we hypothesized that PGC-1α would sensitize ccRCC cells to cytotoxic therapies. To test this hypothesis, we exposed RCC4 cells to doxorubicin and found that ectopic expression of PGC-1α sensitized ccRCC cells to doxorubicin treatment (Figures 3F). Consistent with this result, RCC4 cells transduced with PGC-1α exhibited a significant decrease in clonogenic survival compared to control (Figure 3G). Similarly, PGC-1α expression dramatically sensitized RCC4 cells to ionizing radiation as measured using the clonogenic survival assay (Figure 3H). These results indicate that therapeutic induction of PGC-1α expression may be an unrecognized mechanism
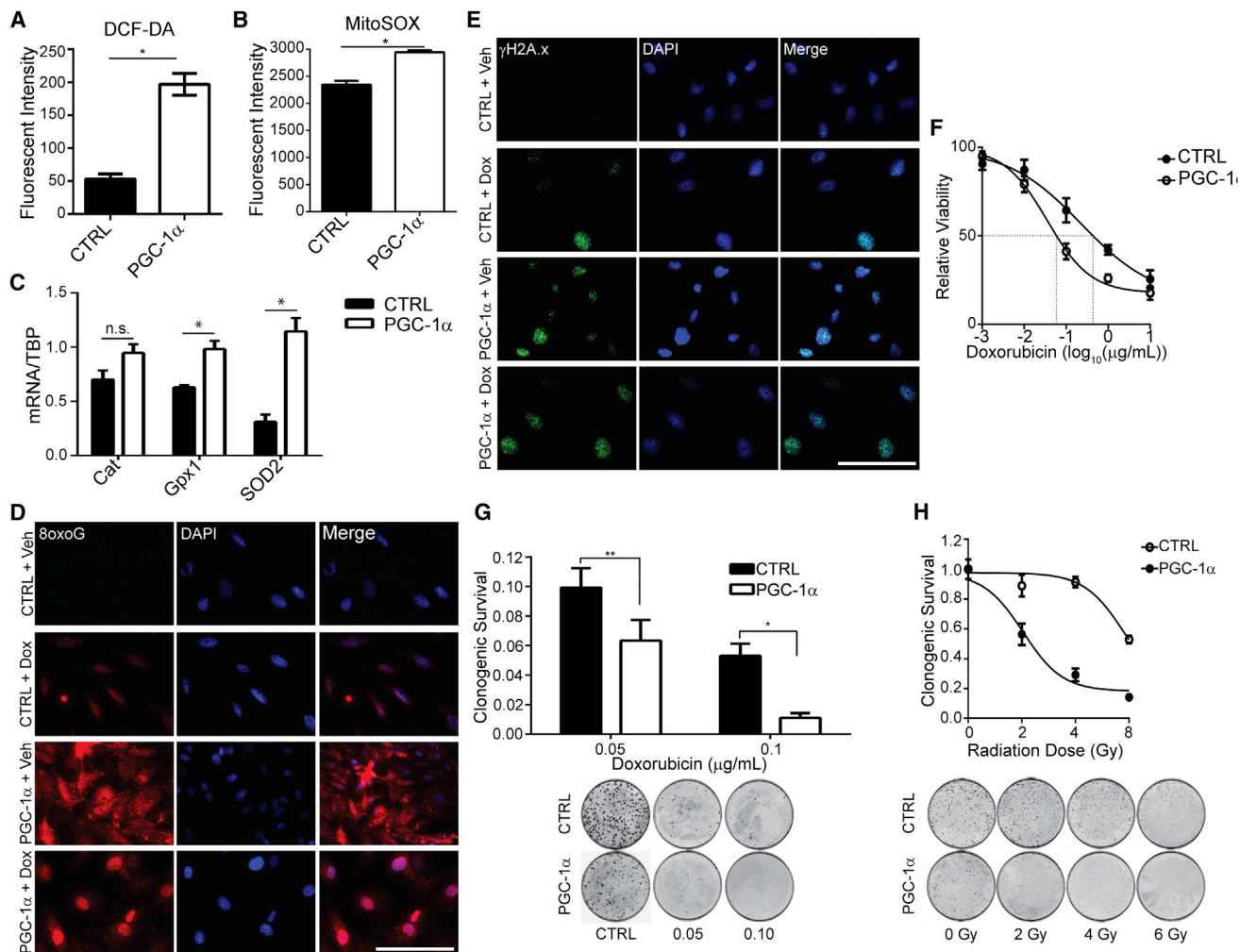
Figure 3. PGC-1α Increases Oxidative Stress in ccRCC and Enhances Sensitivity to Cytotoxic Therapies

(A) Mean DCF-DA staining of control (CTRL) or PGC-1α-transduced RCC4 cells. *p < 0.001 by Student's two-tailed t test.

(B) Mean MitoSOX staining intensity in control or PGC-1α-transduced RCC4 cells. *p < 0.0002 by Student's two-tailed t test.

(C) mRNA levels of the indicated genes in CTRL and PGC-1α-transduced RCC4 cells. *p < 0.025; n.s., p > 0.05 by Student's two-tailed t test.

(D) 8-hydroxyguanosine (8oxoG) immunofluorescent (IF) staining of CTRL and PGC-1α-transduced RCC4 cells treated with vehicle (Veh) or 0.1 μg/ml doxorubicin (Dox) for 48 hr. Scale bar, 100 μm.

(E) Phosphorylated histone H2A.x (Ser 139) (γH2AX) IF staining of CTRL and PGC-1α-transduced RCC4 cells treated with Veh or Dox for 48 hr. Scale bar, 100 μm.

(F) XTT assay of CTRL and PGC-1α-transduced RCC4 cells treated with the indicated dose of doxorubicin for 48 hr. Half maximal inhibitory concentration for doxorubicin killing indicated by a dashed line (CTRL = 0.23 μM, PGC-1α = 0.04 μM).

(G) Clonogenic survival of CTRL and PGC-1α-transduced RCC4 cells treated with the indicated concentration of doxorubicin. *p < 0.02; **p = 0.01 by Student's two-tailed t test.

(H) Clonogenic survival of CTRL and PGC-1α-transduced RCC4 cells treated with 0, 2, 4, or 6 Gy ionizing radiation.

All bar graphs are plotted as mean ± SD. See also Figure S4.

to enhance the efficacy of chemotherapy and radiotherapy in the treatment of ccRCC.

HIF-α-Dependent Suppression of PGC-1α in VHL Deficiency and Hypoxia

To further assess the potential of PGC-1α induction as a therapeutic modality in ccRCC, we sought to characterize the molecular mechanisms underlying suppression of PGC-1α in ccRCC. The tumor suppressor function of VHL is tightly linked with its

ability to regulate the stability of HIF-1α and HIF-2α. To determine whether PGC-1α suppression in VHL-deficient ccRCC cells required HIF-α expression, we used small hairpin RNAs (shRNAs) to target expression of either HIF-1α or HIF-2α. Indicating an essential role for HIFs in mediating PGC-1α suppression, knockdown of either HIF-1α or HIF-2α resulted in increased PGC-1α expression in VHL-deficient RCC4 and 786-O cells, indicating that HIF-α expression is required for suppression of PGC-1α (Figures 4A, 4B, and S5A). We further probed the role of HIF

transcriptional regulatory activity in PGC-1α suppression by assessing whether the obligate HIF-α binding partner, ARNT, was required for PGC-1α suppression. Consistent with the results from HIF-1α and HIF-2α knockdown, suppression of ARNT resulted in increased levels of PGC-1α protein and mRNA in VHL-deficient cells (Figures 4C, 4D, and S5B). These results demonstrate that a functional HIF-α/ARNT transcriptional complex is required for suppression of PGC-1α in VHL-deficient ccRCC.

Although prevalent in ccRCC, VHL loss-of-function mutations are rare in most tumor types. In contrast, hypoxia is a nearly ubiquitous characteristic of solid tumors. To determine whether HIF-dependent regulation of PGC-1α is intact in VHL wild-type cells exposed to low oxygen tensions, we compared expression of PGC-1α protein and mRNA in cell lines cultured in normoxia or hypoxia. Consistent with our results in VHL-deficient cells, hypoxia suppressed PGC-1α protein and mRNA levels in both non-transformed HK2 proximal tubule cells and in VHL wild-type TK10 ccRCC cells (Figures 4E and 4F). When compared to normoxia counterparts, knockdown of HIF-1α blunted the decrease in PGC-1α mRNA and protein in cells exposed to hypoxia, indicating that this effect was HIF dependent (Figures 4G, 4H, and S5C). Similarly, HIF-α stabilization induced by treatment with the prolyl hydroxylase inhibitor dimethyloxaloylglycine (DMOG) resulted in HIF-1α-dependent suppression of PGC-1α mRNA (Figure 4I). Treatment with DMOG also resulted in HIF-1α-dependent inhibition of *Ppargc1a* promoter activity, indicating that diminished expression of PGC-1α likely occurs at least in part through transcriptional repression (Figure 4J). These results demonstrate that PGC-1α transcription is inhibited in a HIF-dependent manner in ccRCC.

Dec1 Is Necessary and Sufficient for Transcriptional Repression of PGC-1α

Although hypoxia is associated with widespread changes in gene expression, including both induction and repression of numerous genes, HIF-1α and HIF-2α function exclusively as transcriptional activators of their direct target genes (Schödel et al., 2011). We thus hypothesized that a transcriptional repressor must function as an intermediate in PGC-1α suppression. The basic-helix-loop-helix transcription factor Dec1 (Stra13/Bhlhe40) is a hypoxia-inducible gene that acts as a transcriptional repressor (Sun and Taneja, 2000). Interestingly, Dec1 has previously been reported to suppress PPARγ2 during adipocyte differentiation and PGC-1α during myogenesis (Hsiao et al., 2009; Yun et al., 2002). We thus hypothesized that Dec1 acts downstream of HIF stabilization to functionally suppress PGC-1α in ccRCC.

In support of this hypothesis, Dec1 expression was inversely correlated with PGC-1α in ccRCC and normal kidney samples (Figure 5A). Dec1 protein levels were elevated in VHL-deficient ccRCC cell lines, and suppression of Dec1 in these cells increased PGC-1α mRNA and protein levels (Figures 5B–5D). In VHL wild-type cells, DMOG treatment increased Dec1 protein levels while decreasing PGC-1α protein levels (Figure 5E). Consistent with an essential role for Dec1 as an effector of HIF-mediated PGC-1α suppression, genetic inhibition of Dec1 abrogated suppression of PGC-1α expression in hypoxia (Figure 5F). Additionally, in VHL wild-type TK10 cells, inhibition of *Ppargc1a* promoter activity by DMOG treatment required

expression of Dec1 (Figure 5G). Phylogenetic analysis of the *Ppargc1a* promoter revealed two highly conserved putative Dec1 binding sites, indicating the evolutionary importance of Dec1-mediated regulation of PGC-1α (Figures S5D–S5F). To examine whether Dec1 could suppress PGC-1α in the absence of HIF-activation, we ectopically expressed Dec1 in TK10 cells and found that Dec1 expression was sufficient to suppress PGC-1α (Figure 5H). Together, these results indicate that Dec1 is necessary and sufficient for suppression of PGC-1α in ccRCC and provide a mechanistic link between HIF, the predominant oncogenic driver of ccRCC, and PGC-1α.

PGC-1α Expression Suppresses ccRCC Tumor Growth

Given our finding that ectopic PGC-1α expression stimulates oxidative stress in ccRCC cells, we hypothesized that restored expression of PGC-1α could suppress ccRCC growth. Supporting this hypothesis, PGC-1α expression inhibited growth of two VHL-deficient ccRCC cell lines in vitro (Figures 6A and 6B). Consistent with the anti-proliferative effects of PGC-1α expression in vitro, subcutaneous growth of 786-O tumors was significantly impaired by expression of PGC-1α (Figures 6C and S6). Furthermore, PGC-1α-transduced 786-O tumors were characterized by an apparent reduction in the clear cell morphology (Figure 6D). Consistent with our in vitro data indicating that PGC-1α expression is sufficient to stimulate increased mitochondrial content, immunohistochemical (IHC) analysis of 786-O tumors revealed increased expression of the mitochondrial protein Tom20 in tumors expressing PGC-1α (Figures 6E). Corroborating our in vitro data that PGC-1α expression induces oxidative stress in ccRCC cells, PGC-1α-transduced tumors exhibited elevated levels of 8oxoG and γH2AX (Figures 6F and 6G). These results indicate that increased expression of PGC-1α inhibits ccRCC growth and highlight the potential of PGC-1α induction as a therapeutic modality in the treatment of ccRCC.

To assess the impact of PGC-1α expression in clinical cases of ccRCC, we next analyzed RNA sequencing data from over 500 patients with ccRCC from the Cancer Genome Atlas (TCGA) to further explore the role of PGC-1α in ccRCC tumorigenesis. These analyses revealed that low expression of PGC-1α was significantly correlated with worse overall survival than patients whose tumors expressed relatively high levels of PGC-1α (Figure 6H). Consistent with these findings, patients harboring tumors with low expression of PGC-1α were significantly more likely to have advanced-stage tumors and metastatic disease (Figure 6I and 6J). Together, these results indicate that low expression of PGC-1α may be a prognostic factor in ccRCC.

DISCUSSION

Our data indicate that PGC-1α is suppressed in *VHL*-deficient ccRCC through HIF-dependent induction of the transcriptional repressor, Dec1. In VHL wild-type proximal tubule cells, PGC-1α suppression disrupts mitochondrial respiration. Conversely, rescued expression of PGC-1α in VHL-deficient ccRCC cell lines restores mitochondrial function in an ERRα-dependent manner. Importantly, the increases in mitochondrial respiration upon expression of PGC-1α are associated with induction of oxidative stress in ccRCC cell lines. In addition to stimulating oxidative
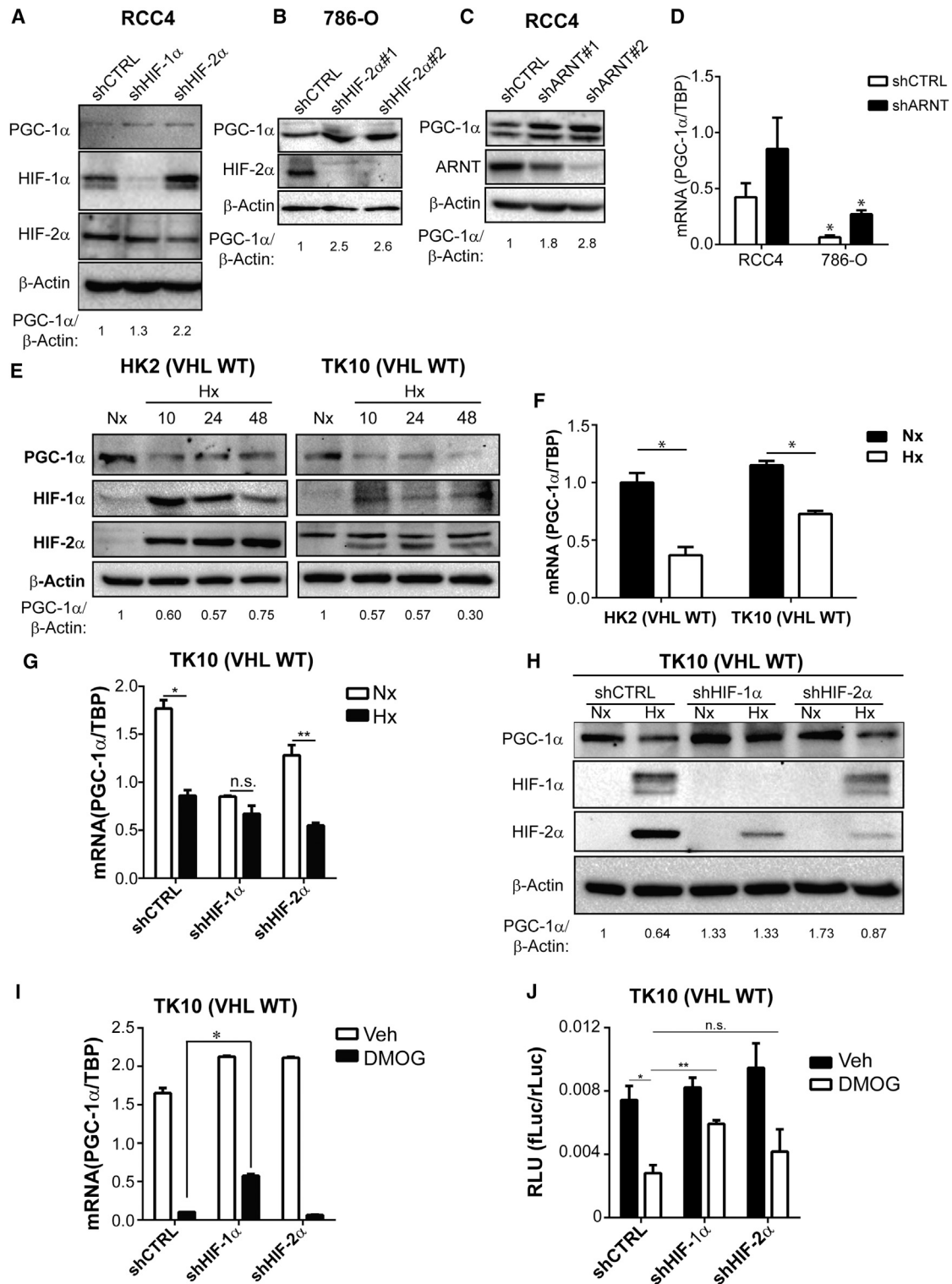
Figure 4. Regulation of PGC-1α Expression by HIF-1α and HIF-2α

(A) Western blots of VHL-deficient RCC4 cells transduced with shCTRL, shHIF-1α, or shHIF-2α

(B) Western blots of VHL-deficient 786-O cells transduced with shCTRL or shHIF-2α.

(C) Western blots of RCC4 cells transduced with shCTRL or shARNT.

(D) PGC-1α mRNA levels in RCC4 and 786-O cells transduced with shCTRL or shARNT. *p < 0.05 by Student's two-tailed t test.

(legend continued on next page)

stress, PGC-1α expression also sensitizes VHL-deficient ccRCC lines to cytotoxic therapies and inhibits in vitro and in vivo growth, highlighting the potential of targeting this pathway in the treatment of ccRCC. In clinical ccRCC datasets, PGC-1α expression is decreased compared to normal renal cortex, and low levels of PGC-1α expression are associated with poor outcome, further indicating that PGC-1α can suppress ccRCC tumorigenesis.

PGC-1α has been reported to have pro- or anti-tumorigenic function in various tumors, but the reasons for this heterogeneous response remain unclear. One possibility is that PGC-1α interacts with different tissue-specific transcription factors, thus driving distinct genetic programs in different cancer types. However, increased mitochondrial biogenesis appears to be a ubiquitous response to PGC-1α expression regardless of the cancer type or outcome of PGC-1α expression. Given this, we postulate that the outcome of PGC-1α expression on tumor growth is likely dictated at least in part by whether the genetic landscape or tumor microenvironment are permissive to increased mitochondrial activity. For example, LeBleu et al. report increased PGC-1α in circulating tumor cells (CTCs) relative to the primary orthotopic tumor. One could reasonably expect the metabolic demands of CTCs in the oxygen-rich circulatory system to be different from a hypoxic cancer cell. In the case of ccRCC, the increased production of ROS upon expression of PGC-1α is inadequately detoxified, leading to oxidative stress. Whether the antioxidant response dictates outcome to enhanced mitochondrial biogenesis downstream of PGC-1α activation will require further investigation.

PGC-1α expression is induced in a subset of melanomas where its expression is regulated by MITF (Haq et al., 2013; Vazquez et al., 2013). Interestingly, hypoxia negatively regulates MITF expression through induction of Dec1, the same transcriptional repressor implicated in our studies as a repressor of PGC-1α (Feige et al., 2011). These results suggest that the tumor microenvironment could play a meaningful role in dictating tumor response to PGC-1α expression. Future studies will be needed to fully understand the mechanisms underlying these differences in tumor response to PGC-1α and the clinical implications thereof.

Here, we demonstrate that restored expression of PGC-1α increases mitochondrial content, ROS production, and oxidative damage, with the ultimate effect of impaired tumor growth and enhanced therapeutic response. ccRCC tumors are typically refractory to cytotoxic chemotherapy and radiotherapy, but the induction of PGC-1α may present an opportunity to enhance efficacy and improve the treatment of ccRCC. Despite the apparent difficulties associated with targeting transcription factors, several groups have conducted high-throughput screens that have identified both transcriptional and post-translational activators of PGC-1α (Arany et al., 2008; Lee et al., 2014). In the future, it will be important to determine whether the pharmacological activation of PGC-1α, either through increasing PGC-1α expression or activating the existing pool of endogenous PGC-1α, is a viable therapeutic modality for the treatment of ccRCC.

EXPERIMENTAL PROCEDURES

Cell Culture

Cells were cultured in DMEM + 10% complete or charcoal-stripped fetal bovine serum (FBS) where indicated. Human PGC-1α cDNA was ectopically expressed by retroviral transduction using the pLPC vector. All shRNA constructs other than shHIF-1α (pSIREN) were in pLKO.1 vector and were purchased from Open Biosystems. Cell viability was assessed by XTT assay as described previously (Turcotte et al., 2008). For clonogenic assays, cells were pre-treated for 48 hr with the indicated dose of doxorubicin or irradiated with the indicated dose of ionizing radiation, cultured for 10 days, and stained with crystal violet to visualize colonies. Clonogenic survival was determined by dividing the number of surviving colonies by the number of cells plated. For siRNA experiments, ON-TARGETplus siRNA SMARTpools containing four siRNAs were purchased from Dharmacon. siRNAs were transfected into cells using Dharmafect1 transfection reagent (Dharmacon), and cells were collected for gene expression analysis or extracellular flux analysis 48 hr post-transfection. All cell lines used in these studies have been previously described elsewhere (Bear et al., 1987; Maxwell et al., 1999; Ryan et al., 1994).

Extracellular Flux Analysis

OCR/ECAR measurements were performed using XF96 extracellular flux analyzer (Seahorse Biosciences). Experiments were conducted in DMEM with 5% FBS, 25 mM glucose, 2 mM glutamine, and 1 mM pyruvate, but without $NaHCO_3$. Inhibitors were injected to final concentrations of 2.5 μg/ml oligomycin, 5 μM FCCP, 2.5 μM antimycin A, 1 μM rotenone, and 100 μM etomoxir. All chemicals were purchased from Sigma-Aldrich.

GC-MS Metabolomics

Cell pellets were extracted with 0.45 ml water/methanol (1:1 volume, containing 20 μM L-norvaline) and 0.225 ml chloroform containing 4 μg/ml heptadecanoic acid as described in detail before (Ratnikov et al., 2015; Scott et al., 2011). Polar metabolites extracted into the water/methanol phase were derivatized and analyzed by GC-MS.

Luciferase Assays

A 1.8 kb region of the proximal *Ppargc1a* promoter was cloned from HK2 cells into the pGL3-basic reporter plasmid (Promega). TK10 cells were transiently transfected with this construct along with cytomegalovirus (CMV)-Renilla reporter to monitor transfection efficiency. Firefly and Renilla

---

(E) Western blots of VHL wild-type HK2 and TK10 cells cultured in normoxia (21% O_2 [Nx]) or hypoxia (0.5% O_2 [Hx]) for the indicated time (hr).

(F) PGC-1α mRNA levels in HK2 and TK10 cells cultured in normoxia (21% O_2 [Nx]) or hypoxia (0.5% O_2 [Hx]) for 24 hr. *p < 0.01 by Student's two-tailed t test.

(G) PGC-1α mRNA levels in TK10 cells transduced with shCTRL, shHIF-1α, or shHIF-2α shRNA constructs and cultured in normoxia (21% O_2 [Nx]) or hypoxia (0.5% O_2 [Hx]) for 24 hr. *p < 0.0005; **p < 0.001; n.s., p > 0.06 by Student's two-tailed t test.

(H) Western blots of TK10 cells transduced with shCTRL, shHIF-1α, or shHIF-2α and cultured in normoxia (21% O_2, Nx) or hypoxia (0.5% O_2, Hx) for 24 hr.

(I) PGC-1α mRNA levels in TK10 cells transduced with shCTRL, shHIF-1α, or shHIF-2α shRNA constructs and treated with 1 mM DMOG or vehicle control (CTRL) for 24 hr. *p < 0.001 by Student's two-tailed t test.

(J) *Ppargc1a* promoter reporter activity (firefly luciferase/CMV-Renilla luciferase activity [RLU]) in TK10 cells transduced with control, shCTRL, shHIF-1α, or shHIF-2α and cultured in vehicle (Veh) or 1 mM DMOG for 18 hr. Two-tailed Student's t test results: *shCTRL Veh versus shCTRL DMOG: p < 0.05; **shCTRL DMOG versus shHIF-1α DMOG: p < 0.005; n.s., shCTRL DMOG versus shHIF-2α DMOG: p = 0.23.

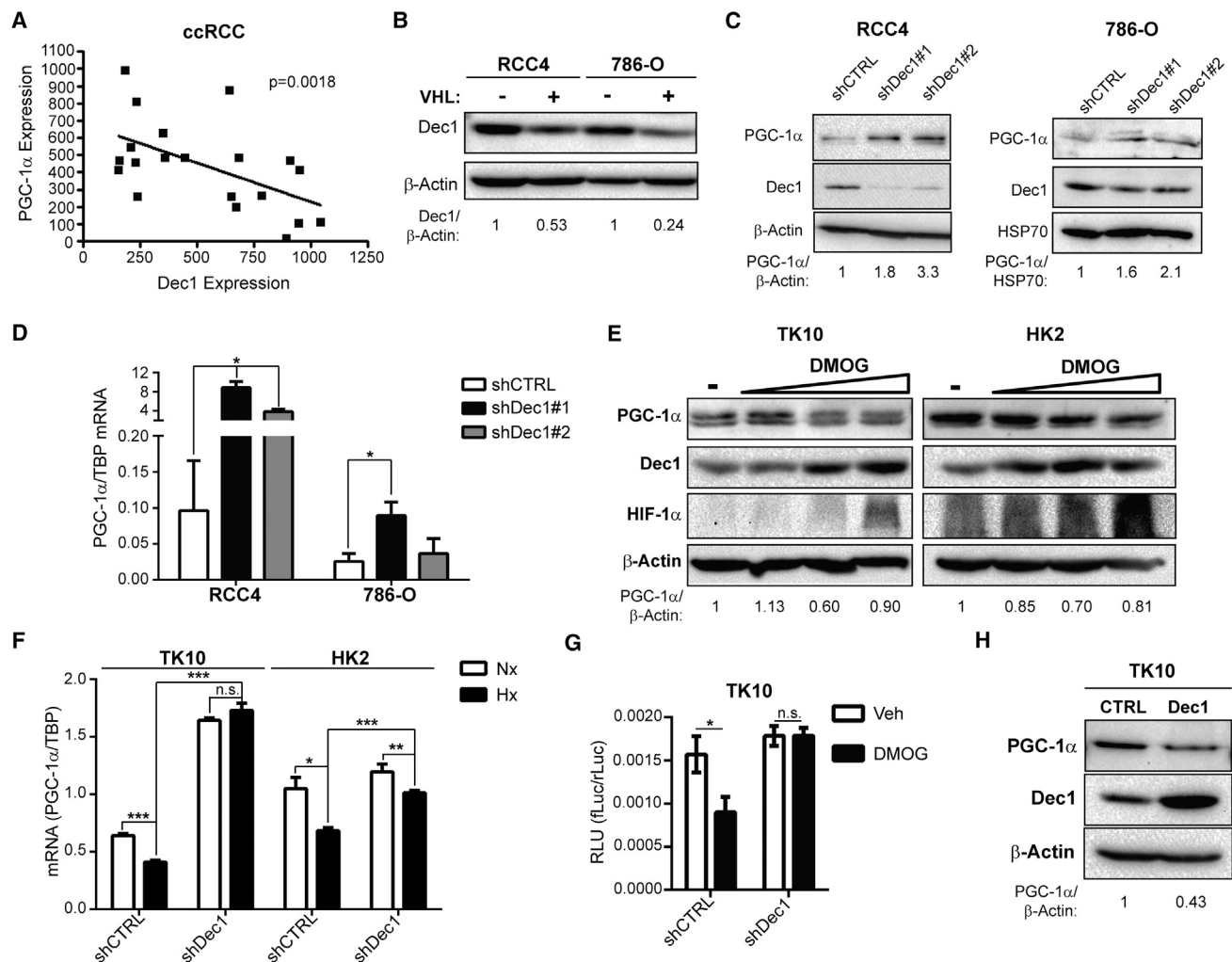All bar graphs are plotted as mean ± SD. See also Figure S5.

Figure 5. Dec1 Is Necessary and Sufficient for Transcriptional Suppression of PGC-1α

(A) mRNA expression of PGC-1α and Dec1 in renal cortex and ccRCC tumors. GEO accession number GEO:GSE6344. Pearson correlation co-efficient ρ = −0.55, two-tailed t test p = 0.0018.

(B) Western blots of VHL-deficient (−VHL) or wild-type (+VHL) RCC4 and 786-O cells.

(C) Western blots of RCC4 and 786-O cells transduced with shCTRL or shDec1.

(D) PGC-1α mRNA levels in RCC4 and 786-O cells transduced with shCTRL or shDec1. *p = 0.01 by Student's two-tailed t test shDec1 versus shCTRL.

(E) Western blots of VHL wild-type HK2 and TK10 cells treated with vehicle or 0.1, 0.5, or 1 mM DMOG for 24 hr.

(F) PGC-1α mRNA levels in TK10 and HK2 cells transduced with shCTRL or shDec1 and cultured in normoxia (Nx) or hypoxia (Hx) for 24 hr. *p = 0.017; **p < 0.05; ***p ≤ 0.0001.; n.s. p > 0.05 by Student's two-tailed t test.

(G) *Ppargc1a* promoter reporter activity (firefly luciferase/CMV-Renilla luciferase activity [RLU]) in vehicle- (Veh) and DMOG-treated (1 mM) TK10 cells transduced with shCTRL or shDec1. *p < 0.02; n.s., p > 0.05 by Student's two-tailed t test.

(H) Western blots of TK10 cells ectopically expressing Dec1.

All bar graphs are plotted as mean ± SD. See also Figure S5.

luciferase levels were quantified with Bright-Glo and Renilla luciferase assays (Promega).

Microarray and RNA-Sequencing Analysis

GEO:GSE6344 and GEO:GSE15641 were selected for analysis from the GEO database due to the representation of both normal renal cortex and ccRCC specimens within each dataset (Gumz et al., 2007; Jones et al., 2005; Tun et al., 2010). For GEO:GSE15641, data from non-ccRCC subtypes of kidney cancer were excluded from our analysis. Datasets were analyzed using the GSEA module in the GenePattern software suite (Reich et al., 2006; Subrama-

nian et al., 2005). Microarrays comparing expression changes in VHL-deficient and wild-type RCC4 cells and after culture of RCC4+VHL cells in hypoxia have been previously described (Krieg et al., 2010). Differentially expressed genes above or below a fold change threshold (>1.5-fold or < −1.5-fold) in both datasets were analyzed using the DAVID functional annotation tool (Huang et al., 2009a, 2009b).

Ppargc1a expression levels were extracted from level 3 RNA-sequencing data from the KIRC TCGA dataset using the "normalized_count" parameter (https://tcga-data.nci.nih.gov/tcga/) and matched by TCGA barcode with corresponding clinical information including time to death or last follow-up,
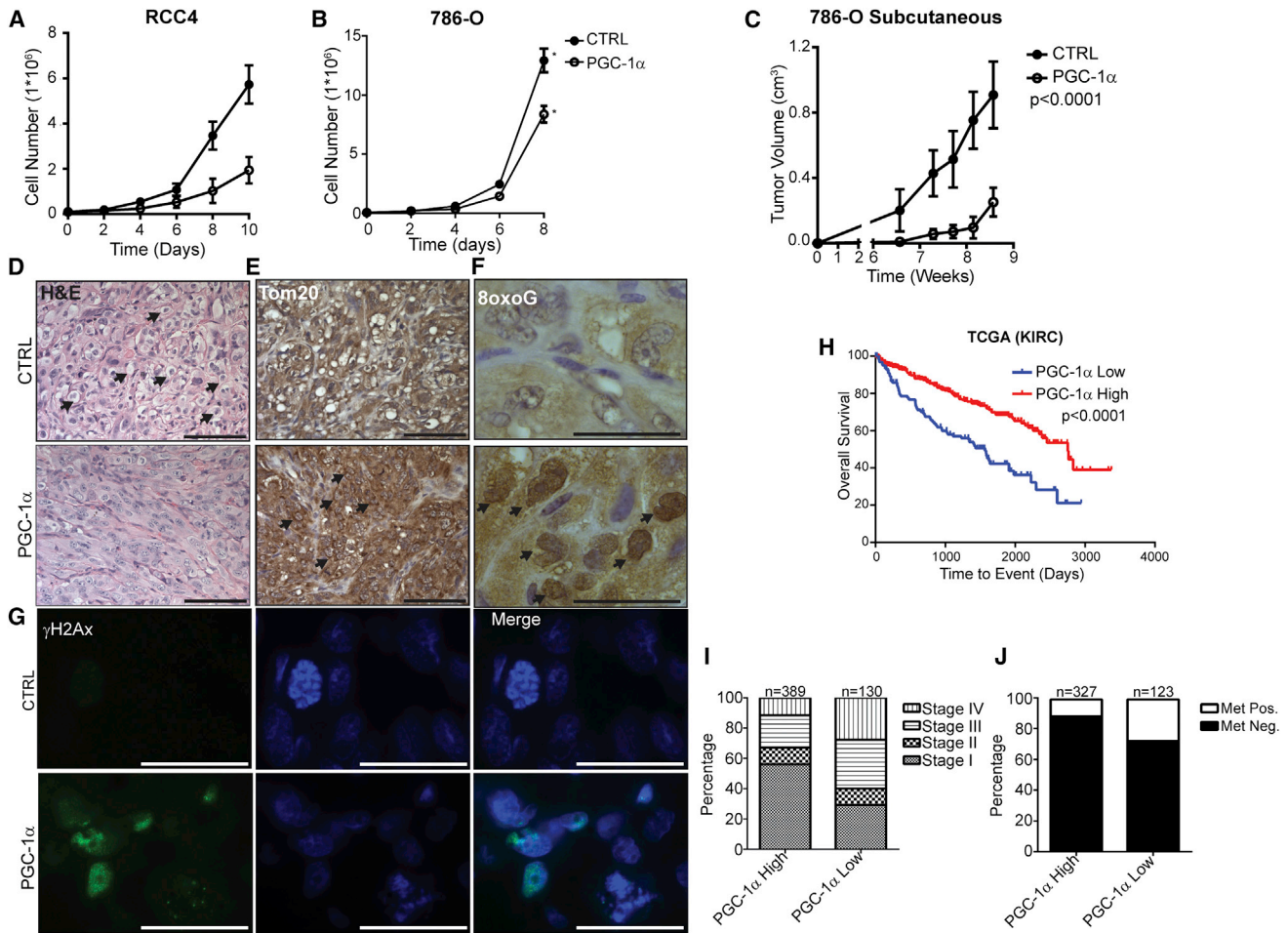
Figure 6. PGC-1α Suppresses ccRCC Growth

(A) In vitro growth curves of CTRL or PGC-1α-transduced RCC4 cells.

(B) In vitro growth curves of CTRL or PGC-1α-transduced 786-O cells. *p < 0.05 by Student's two-tailed t test.

(C) Subcutaneous tumor volume of CTRL or PGC-1α-transduced 786-O cells. Mixed-effects model p < 0.0001 between CTRL and PGC-1α.

(D) H&E-stained CTRL or PGC-1α-transduced 786-O subcutaneous tumors. Arrows denote cells with evident clear cell morphology. Scale bar, 100 μm.

(E) Tom20 immunohistochemical (IHC) staining of CTRL or PGC-1α-transduced 786-O subcutaneous tumors. Arrows denote cells with strong perinuclear Tom20 staining. Scale bar, 100 μm.

(F) 8oxoG IHC staining of CTRL or PGC-1α-transduced 786-O subcutaneous tumors. Arrows denote nuclei with strongly positive 8oxoG staining. Scale bar, 25 μm.

(G) γH2Ax IF staining of CTRL or PGC-1α-transduced 786-O subcutaneous tumors. Nuclei were counterstained with DAPI. Scale bar, 25 μm.

(H) Kaplan-Meier Curve for ccRCC patients segregated by low (bottom quartile) or high expression of PGC-1α. Log-rank test p < 0.0001.

(I) Percentage of patients with AJCC stage I–IV disease, segregated by PGC-1α expression as in (H).

(J) Percentage of patients with detectable metastases. Patients are segregated by PGC-1α expression as in (H).

All bar graphs are presented as mean ± SD. See also Figure S6.

American Joint Committee on Cancer tumor staging, and the presence or absence of metastatic disease. To segregate patients according to high or low expression of PGC-1α, the median expression from all patients in the dataset was calculated and patients were segregated into the PGC-1α-low group if PGC-1α expression in the tumor was in the bottom quartile of expression. The remaining patients were included in the PGC-1α-high group.

Microscopy and Immunohistochemistry

For fluorescent labeling of mitochondria, live cells were incubated with 100 nM CMXROS (Molecular Probes) in buffer containing 100 mM KCl to depolarize the mitochondrial membrane for 30 min at 37°C. Antibodies used for IHC and immunofluorescence experiments were 8-hydroxyguanosine (Abcam),

γH2AX (Millipore), and Tom20 (Santa Cruz). For IHC experiments, primary antibody labeling was detected after incubation with the appropriate secondary antibody by incubation with 3, 3′-diaminobenzidine (DAB; Vector Labs). For IF experiments, nuclei were counterstained for 5 min with DAPI. For IHC staining experiments, slides were counterstained with hematoxylin.

Quantitative Real-Time PCR

mRNA was extracted from cells using Trizol (Invitrogen) and reverse transcribed using Superscript II reverse transcriptase (Invitrogen). Relative mRNA levels were calculated using the standard curve methodology. For mtDNA quantification, total DNA was isolated from cultured cells using phenol/chloroform/isoamyl alcohol (Invitrogen). Primers were designed to

amplify the 16S rRNA gene from the mtDNA genome and were normalized to the nuclear gene β2-microglobulin. A complete list of primer sets can be found in Table S1.

ROS Measurements

Live cells were stained with either DCF-DA or MitoSOX stains according to manufacturer-recommended protocol. Briefly, cells were incubated with 10 μM DCF-DA (Molecular Probes) or 5 μM MitoSOX Red (Life Technologies) for 30 min at 37°C. After PBS wash, cells were analyzed by flow cytometry using an LSRII flow cytometer (Becton Dickenson).

Western Blotting

Western blot images were acquired using the ChemiDoc CCD imaging system (Bio-Rad). The following antibodies were used for western blotting: ARNT (Novus), β-actin (Sigma-Aldrich), Dec1 (Novus), HIF-1α (BD), HIF-2α (Novus), HSP70 (Sigma-Aldrich), PGC-1α (Sigma-Aldrich and Santa Cruz), and Tfam (Sigma-Aldrich). Densitometry analysis was performed using ImageJ software, and relative values were calculated by normalizing to the control group from each experiment (Schneider et al., 2012).

Xenograft Tumor Growth

5×10^6 control (CTRL) or PGC-1α-transduced 786-O cells were injected into the flanks of non-obese diabetic/severe combined immunodeficiency mice (n = 5 for control group, n = 8 for PGC-1α group). Tumor size was measured weekly, and volume was calculated according to the following formula: volume = (width^2 × length) ÷ 2.

Because the tumor volumes of the mice in both treatment groups (CTRL and PGC-1α) followed a log-normal distribution, the data were log transformed to render the data normally distributed and to analyze the data in a mixed-effects model. The data were analyzed in a mixed-effects model to accommodate the repeated measure of tumor volume over time. The effect of treatment was included as a fixed effect in the model, and day was included as a random effect. The variance-covariance matrix was assumed to have a compound symmetry structure. In the final model, the treatment effect (CTRL versus PGC-1α) was significant (treatment p < 0.0001).

All animal experiments were conducted in accordance with standard institutional animal care and use committee protocols.

SUPPLEMENTAL INFORMATION

Supplemental Information includes seven figures and one table can be found with this article online at http://dx.doi.org/10.1016/j.celrep.2015.06.006.

AUTHOR CONTRIBUTIONS

E.L.L. and A.J.G. designed all experiments, wrote and revised the manuscript, and shared oversight of this project. E.L.L. performed and analyzed data for most experiments. C.W. provided critical assistance with in vivo tumor growth studies and revised the manuscript. C.M.T. performed cloning of PGC-1α constructs. C.-K.C.D. and J.-T.C. assisted with bioinformatics analysis, including analysis of Ppargc1a expression in ccRCC GEO datasets. D.A.S. and A.D.R. assisted in experimental design and execution of GC-MS analysis of TCA cycle metabolite abundance. R.v.E. assisted with statistical analysis of 786-O xenograft studies.

REFERENCES

Arany, Z., Wagner, B.K., Ma, Y., Chinsomboon, J., Laznik, D., and Spiegelman, B.M. (2008). Gene expression-based screening identifies microtubule inhibitors as inducers of PGC-1alpha and oxidative phosphorylation. Proc. Natl. Acad. Sci. USA 105, 4721–4726.

Bear, A., Clayman, R.V., Elbers, J., Limas, C., Wang, N., Stone, K., Gebhard, R., Prigge, W., and Palmer, J. (1987). Characterization of two human cell lines (TK-10, TK-164) of renal cell cancer. Cancer Res. 47, 3856–3862.

Cancer Genome Atlas Research Network (2013). Comprehensive molecular characterization of clear cell renal cell carcinoma. Nature 499, 43–49.

D'Errico, I., Salvatore, L., Murzilli, S., Lo Sasso, G., Latorre, D., Martelli, N., Egorova, A.V., Polishuck, R., Madeyski-Bengtson, K., Lelliott, C., et al. (2011). Peroxisome proliferator-activated receptor-gamma coactivator 1-alpha (PGC1alpha) is a metabolic regulator of intestinal epithelial cell fate. Proc. Natl. Acad. Sci. USA 108, 6603–6608.

Feige, E., Yokoyama, S., Levy, C., Khaled, M., Igras, V., Lin, R.J., Lee, S., Widlund, H.R., Granter, S.R., Kung, A.L., and Fisher, D.E. (2011). Hypoxia-induced transcriptional repression of the melanoma-associated oncogene MITF. Proc. Natl. Acad. Sci. USA 108, E924–E933.

Fukuda, R., Zhang, H., Kim, J.W., Shimoda, L., Dang, C.V., and Semenza, G.L. (2007). HIF-1 regulates cytochrome oxidase subunits to optimize efficiency of respiration in hypoxic cells. Cell 129, 111–122.

Gnarra, J.R., Tory, K., Weng, Y., Schmidt, L., Wei, M.H., Li, H., Latif, F., Liu, S., Chen, F., Duh, F.M., et al. (1994). Mutations of the VHL tumour suppressor gene in renal carcinoma. Nat. Genet. 7, 85–90.

Gordan, J.D., and Simon, M.C. (2007). Hypoxia-inducible factors: central regulators of the tumor phenotype. Curr. Opin. Genet. Dev. 17, 71–77.

Gumz, M.L., Zou, H., Kreinest, P.A., Childs, A.C., Belmonte, L.S., LeGrand, S.N., Wu, K.J., Luxon, B.A., Sinha, M., Parker, A.S., et al. (2007). Secreted frizzled-related protein 1 loss contributes to tumor phenotype of clear cell renal cell carcinoma. Clin. Cancer Res. 13, 4740–4749.

Hanahan, D., and Weinberg, R.A. (2011). Hallmarks of cancer: the next generation. Cell 144, 646–674.

Haq, R., Shoag, J., Andreu-Perez, P., Yokoyama, S., Edelman, H., Rowe, G.C., Frederick, D.T., Hurley, A.D., Nellore, A., Kung, A.L., et al. (2013). Oncogenic BRAF regulates oxidative metabolism via PGC1α and MITF. Cancer Cell 23, 302–315.

Hsiao, S.P., Huang, K.M., Chang, H.Y., and Chen, S.L. (2009). P/CAF rescues the Bhlhe40-mediated repression of MyoD transactivation. Biochem. J. 422, 343–352.

Huang, W., Sherman, B.T., and Lempicki, R.A. (2009a). Bioinformatics enrichment tools: paths toward the comprehensive functional analysis of large gene lists. Nucleic Acids Res. 37, 1–13.

Huang, W., Sherman, B.T., and Lempicki, R.A. (2009b). Systematic and integrative analysis of large gene lists using DAVID bioinformatics resources. Nat. Protoc. 4, 44–57.

Ivan, M., Kondo, K., Yang, H., Kim, W., Valiando, J., Ohh, M., Salic, A., Asara, J.M., Lane, W.S., and Kaelin, W.G., Jr. (2001). HIFalpha targeted for VHL-mediated destruction by proline hydroxylation: implications for O2 sensing. Science 292, 464–468.

Jaakkola, P., Mole, D.R., Tian, Y.M., Wilson, M.I., Gielbert, J., Gaskell, S.J., von Kriegsheim, A., Hebestreit, H.F., Mukherji, M., Schofield, C.J., et al. (2001). Targeting of HIF-alpha to the von Hippel-Lindau ubiquitylation complex by O2-regulated prolyl hydroxylation. Science 292, 468–472.

Jones, J., Otu, H., Spentzos, D., Kolia, S., Inan, M., Beecken, W.D., Fellbaum, C., Gu, X., Joseph, M., Pantuck, A.J., et al. (2005). Gene signatures of progression and metastasis in renal cell cancer. Clin. Cancer Res. 11, 5730–5739.

Kondo, K., Klco, J., Nakamura, E., Lechpammer, M., and Kaelin, W.G., Jr. (2002). Inhibition of HIF is necessary for tumor suppression by the von Hippel-Lindau protein. Cancer Cell 1, 237–246.

Krieg, A.J., Rankin, E.B., Chan, D., Razorenova, O., Fernandez, S., and Giaccia, A.J. (2010). Regulation of the histone demethylase JMJD1A by hypoxia-inducible factor 1 alpha enhances hypoxic gene expression and tumor growth. Mol. Cell. Biol. 30, 344–353.

Krishnan, J., Danzer, C., Simka, T., Ukropec, J., Walter, K.M., Kumpf, S., Mirtschink, P., Ukropcova, B., Gasperikova, D., Pedrazzini, T., and Krek, W. (2012). Dietary obesity-associated Hif1α activation in adipocytes restricts fatty acid oxidation and energy expenditure via suppression of the Sirt2-NAD+ system. Genes Dev. 26, 259–270.

LeBleu, V.S., O'Connell, J.T., Gonzalez Herrera, K.N., Wikman, H., Pantel, K., Haigis, M.C., de Carvalho, F.M., Damascena, A., Domingos Chinen, L.T., Rocha, R.M., et al. (2014). PGC-1α mediates mitochondrial biogenesis and oxidative phosphorylation in cancer cells to promote metastasis. Nat. Cell Biol. 16, 992–1003, 1–15.

Lee, Y., Dominy, J.E., Choi, Y.J., Jurczak, M., Tolliday, N., Camporez, J.P., Chim, H., Lim, J.H., Ruan, H.B., Yang, X., et al. (2014). Cyclin D1-Cdk4 controls glucose metabolism independently of cell cycle progression. Nature 510, 547–551.

Leone, T.C., Lehman, J.J., Finck, B.N., Schaeffer, P.J., Wende, A.R., Boudina, S., Courtois, M., Wozniak, D.F., Sambandam, N., Bernal-Mizrachi, C., et al. (2005). PGC-1alpha deficiency causes multi-system energy metabolic derangements: muscle dysfunction, abnormal weight control and hepatic steatosis. PLoS Biol. 3, e101.

Lim, J.H., Luo, C., Vazquez, F., and Puigserver, P. (2014). Targeting mitochondrial oxidative metabolism in melanoma causes metabolic compensation through glucose and glutamine utilization. Cancer Res. 74, 3535–3545.

Lin, J., Wu, P.H., Tarr, P.T., Lindenberg, K.S., St-Pierre, J., Zhang, C.Y., Mootha, V.K., Jäger, S., Vianna, C.R., Reznick, R.M., et al. (2004). Defects in adaptive energy metabolism with CNS-linked hyperactivity in PGC-1alpha null mice. Cell 119, 121–135.

Linehan, W.M., Srinivasan, R., and Schmidt, L.S. (2010). The genetic basis of kidney cancer: a metabolic disease. Nat Rev Urol 7, 277–285.

Maxwell, P.H., Wiesener, M.S., Chang, G.W., Clifford, S.C., Vaux, E.C., Cockman, M.E., Wykoff, C.C., Pugh, C.W., Maher, E.R., and Ratcliffe, P.J. (1999). The tumour suppressor protein VHL targets hypoxia-inducible factors for oxygen-dependent proteolysis. Nature 399, 271–275.

Mootha, V.K., Handschin, C., Arlow, D., Xie, X., St Pierre, J., Sihag, S., Yang, W., Altshuler, D., Puigserver, P., Patterson, N., et al. (2004). Erralpha and Gabpa/b specify PGC-1alpha-dependent oxidative phosphorylation gene expression that is altered in diabetic muscle. Proc. Natl. Acad. Sci. USA 101, 6570–6575.

O'Hagan, K.A., Cocchiglia, S., Zhdanov, A.V., Tambuwala, M.M., Cummins, E.P., Monfared, M., Agbor, T.A., Garvey, J.F., Papkovsky, D.B., Taylor, C.T., and Allan, B.B. (2009). PGC-1alpha is coupled to HIF-1alpha-dependent gene expression by increasing mitochondrial oxygen consumption in skeletal muscle cells. Proc. Natl. Acad. Sci. USA 106, 2188–2193.

Papandreou, I., Cairns, R.A., Fontana, L., Lim, A.L., and Denko, N.C. (2006). HIF-1 mediates adaptation to hypoxia by actively downregulating mitochondrial oxygen consumption. Cell Metab. 3, 187–197.

Puigserver, P., Wu, Z., Park, C.W., Graves, R., Wright, M., and Spiegelman, B.M. (1998). A cold-inducible coactivator of nuclear receptors linked to adaptive thermogenesis. Cell 92, 829–839.

Ratnikov, B., Aza-Blanc, P., Ronai, Z.A., Smith, J.W., Osterman, A.L., and Scott, D.A. (2015). Glutamate and asparagine cataplerosis underlie glutamine addiction in melanoma. Oncotarget 6, 7379–7389.

Reich, M., Liefeld, T., Gould, J., Lerner, J., Tamayo, P., and Mesirov, J.P. (2006). GenePattern 2.0. Nat. Genet. 38, 500–501.

Rini, B.I., Campbell, S.C., and Escudier, B. (2009). Renal cell carcinoma. Lancet 373, 1119–1132.

Ryan, M.J., Johnson, G., Kirk, J., Fuerstenberg, S.M., Zager, R.A., and Torok-Storb, B. (1994). HK-2: an immortalized proximal tubule epithelial cell line from normal adult human kidney. Kidney Int. 45, 48–57.

Schneider, C.A., Rasband, W.S., and Eliceiri, K.W. (2012). NIH Image to ImageJ: 25 years of image analysis. Nat. Methods 9, 671–675.

Schödel, J., Oikonomopoulos, S., Ragoussis, J., Pugh, C.W., Ratcliffe, P.J., and Mole, D.R. (2011). High-resolution genome-wide mapping of HIF-binding sites by ChIP-seq. Blood 117, e207–e217.

Scott, D.A., Richardson, A.D., Filipp, F.V., Knutzen, C.A., Chiang, G.G., Ronai, Z.A., Osterman, A.L., and Smith, J.W. (2011). Comparative metabolic flux profiling of melanoma cell lines: beyond the Warburg effect. J. Biol. Chem. 286, 42626–42634.

Shoag, J., and Arany, Z. (2010). Regulation of hypoxia-inducible genes by PGC-1 alpha. Arterioscler. Thromb. Vasc. Biol. 30, 662–666.

Simonnet, H., Alazard, N., Pfeiffer, K., Gallou, C., Béroud, C., Demont, J., Bouvier, R., Schägger, H., and Godinot, C. (2002). Low mitochondrial respiratory chain content correlates with tumor aggressiveness in renal cell carcinoma. Carcinogenesis 23, 759–768.

St-Pierre, J., Drori, S., Uldry, M., Silvaggi, J.M., Rhee, J., Jäger, S., Handschin, C., Zheng, K., Lin, J., Yang, W., et al. (2006). Suppression of reactive oxygen species and neurodegeneration by the PGC-1 transcriptional coactivators. Cell 127, 397–408.

Subramanian, A., Tamayo, P., Mootha, V.K., Mukherjee, S., Ebert, B.L., Gillette, M.A., Paulovich, A., Pomeroy, S.L., Golub, T.R., Lander, E.S., and Mesirov, J.P. (2005). Gene set enrichment analysis: a knowledge-based approach for interpreting genome-wide expression profiles. Proc. Natl. Acad. Sci. USA 102, 15545–15550.

Sun, H., and Taneja, R. (2000). Stra13 expression is associated with growth arrest and represses transcription through histone deacetylase (HDAC)-dependent and HDAC-independent mechanisms. Proc. Natl. Acad. Sci. USA 97, 4058–4063.

Trachootham, D., Alexandre, J., and Huang, P. (2009). Targeting cancer cells by ROS-mediated mechanisms: a radical therapeutic approach? Nat. Rev. Drug Discov. 8, 579–591.

Tun, H.W., Marlow, L.A., von Roemeling, C.A., Cooper, S.J., Kreinest, P., Wu, K., Luxon, B.A., Sinha, M., Anastasiadis, P.Z., and Copland, J.A. (2010). Pathway signature and cellular differentiation in clear cell renal cell carcinoma. PLoS ONE 5, e10696.

Turcotte, S., Chan, D.A., Sutphin, P.D., Hay, M.P., Denny, W.A., and Giaccia, A.J. (2008). A molecule targeting VHL-deficient renal cell carcinoma that induces autophagy. Cancer Cell 14, 90–102.

Vazquez, F., Lim, J.H., Chim, H., Bhalla, K., Girnun, G., Pierce, K., Clish, C.B., Granter, S.R., Widlund, H.R., Spiegelman, B.M., and Puigserver, P. (2013). PGC1α expression defines a subset of human melanoma tumors with increased mitochondrial capacity and resistance to oxidative stress. Cancer Cell 23, 287–301.

Wang, G.L., Jiang, B.H., Rue, E.A., and Semenza, G.L. (1995). Hypoxia-inducible factor 1 is a basic-helix-loop-helix-PAS heterodimer regulated by cellular O2 tension. Proc. Natl. Acad. Sci. USA 92, 5510–5514.

Yan, M., Gingras, M.C., Dunlop, E.A., Nouët, Y., Dupuy, F., Jalali, Z., Possik, E., Coull, B.J., Kharitidi, D., Dydensborg, A.B., et al. (2014). The tumor suppressor folliculin regulates AMPK-dependent metabolic transformation. J. Clin. Invest. 124, 2640–2650.

Yun, Z., Maecker, H.L., Johnson, R.S., and Giaccia, A.J. (2002). Inhibition of PPAR gamma 2 gene expression by the HIF-1-regulated gene DEC1/Stra13: a mechanism for regulation of adipogenesis by hypoxia. Dev. Cell 2, 331–341.

Zhang, H., Gao, P., Fukuda, R., Kumar, G., Krishnamachary, B., Zeller, K.I., Dang, C.V., and Semenza, G.L. (2007). HIF-1 inhibits mitochondrial biogenesis and cellular respiration in VHL-deficient renal cell carcinoma by repression of C-MYC activity. Cancer Cell 11, 407–420.